Eur Biophys J (2008) 37:879–891
DOI 10.1007/s00249-008-0299-7

ORIGINAL PAPER

Selectivity in the mechanism of action of antimicrobial mastoparan peptide Polybia-MP1

Marcia Perez dos Santos Cabrera · Sabrina Thais Broggio Costa · Bibiana Monson de Souza · Mario Sérgio Palma · José Roberto Ruggiero · João Ruggiero Neto

Received: 24 October 2007 / Revised: 10 February 2008 / Accepted: 26 February 2008 / Published online: 15 April 2008

Abstract Many potent antimicrobial peptides also present hemolytic activity, an undesired collateral effect for the therapeutic application. Unlike other mastoparan peptides, Polybia-MP1 (IDWKKLLDAAKQIL), obtained from the venom of the social wasp *Polybia paulista*, is highly selective of bacterial cells. The study of its mechanism of action demonstrated that it permeates vesicles at a greater rate of leakage on the anionic over the zwitterionic, impaired by the presence of cholesterol or cardiolipin; its lytic activity is characterized by a threshold peptide to lipid molar ratio that depends on the phospholipid composition of the vesicles. At these particular threshold concentrations, the apparent average pore number is distinctive between anionic and zwitterionic vesicles, suggesting that pores are similarly formed depending on the ionic character of the bilayer. To prospect the molecular reasons for the strengthened selectivity in Polybia-MP1 and its absence in Mastoparan-X, MD simulations were carried out. Both peptides presented amphipathic α-helical structures, as previously observed in Circular Dichroism spectra, with important differences in the extension and stability of the helix; their backbone solvation analysis also indicate a different profile, suggesting that the selectivity of Polybia-MP1 is a consequence of the distribution of the charged and polar residues along the peptide helix, and on how the solvent molecules orient themselves according to these electrostatic interactions. We suggest that the lack of hemolytic activity of Polybia-MP1 is due to the presence and position of Asp residues that enable the equilibrium of electrostatic interactions and favor the preference for the more hydrophilic environment.

Keywords Selectivity · Cationic antimicrobial peptide · Hydrophobicity · Wasp venom mastoparan · Lytic activity and cooperativity · Conformational analysis

Abbreviations

CD	Circular dichroism
CF	Carboxyfluorescein
CL	Cardiolipin
LUV	Large unilamellar vesicles
MD	Molecular dynamics
PC	L-α-phosphatidylcholine
PG	L-α-phosphatidyl-DL-glycerol
PCC	PC/cholesterol mixture
P/L	Peptide to lipid molar ratio
SUV	Small unilamellar vesicles
TFE	Trifluoroethanol

Electronic supplementary material The online version of this article (doi:10.1007/s00249-008-0299-7) contains supplementary material, which is available to authorized users.

M. P. dos Santos Cabrera (✉) · S. T. B. Costa · J. R. Ruggiero · J. Ruggiero Neto
Department of Physics,
IBILCE, São Paulo State University—UNESP,
R: Cristóvão Colombo, 2265,
15054-000 S. José do Rio Preto, SP, Brazil
e-mail: cabrera.marcia@gmail.com

B. M. de Souza · M. S. Palma
Center of Studies of Social Insects,
Institute of Biosciences, São Paulo State University—UNESP,
Av. 24-A, 1515, 13506-900 Rio Claro, SP, Brazil

M. P. dos Santos Cabrera
Department of Physiology and Biophysics,
Institute of Biomedical Sciences, University of São Paulo,
Av. Prof. Lineu Prestes, 1524, Biomédicas I,
room 101A, 05508-900 São Paulo, SP, Brazil

Introduction

Wasp venom peptides belong to the intensively searched field of bioactive peptides, especially those with antimicrobial action and/or mast cell degranulating activity. Antimicrobial peptides are of high interest as substitutes of conventional antibiotics—or promoters of their action—due to the widespread increase in microorganisms' resistance (Zasloff, 2002). Among them, mastoparan peptides present an impressive list of activities (Higashijima et al. 1990; Hirai et al. 1979a, b; Mendes et al. 2005; Nakajima et al. 1986), most of which are clearly related to an amphipathic, cationic structure. The presence of charged and polar residues along the chain displays different possibilities of electrostatic interaction, the longest in range, whose effects in the helix stabilization or destabilization are dependent on their relative position in the chain (Shoemaker et al. 1985). As demonstrated in former experimental work by Dathe et al. (1996, 1997), and recently described in the theoretical model by Taheri-Araghi and Ha (2007), selectivity comes from relationships between electrostatic and hydrophobic interactions. High-charge density requires a larger number of lipids, anionic or zwitterionic, to be counterbalanced, causing shrinkage of the optimal head group area of lipids (Taheri-Araghi and Ha 2007), and leading to pore formation. When this effect is maximized in anionic bilayers and can be minimized in the zwitterionic, a selective mechanism of action will be played.

Polybia-MP1, IDWKKLLDAAKQIL-NH2, isolated from the venom reservoir of social wasp *Polybia paulista* (Souza et al. 2005) presents antimicrobial activity and is not hemolytic. This selective behavior in relation to the nature of the membrane it targets is not shared by the more investigated Mastoparan (MP, from *Vespula lewisii*) Mastoparan-X (MP-X, from *Vespa xanthoptera*) and Mastoparan-B (MP-B, from *Vespa basalis*). Comparing physicochemical characteristics of these mastoparan peptides, the selectivity of Polybia-MP1 was thought to be due to its mean hydrophobicity and the number of charged residues. In the present work, we searched for specificity in peptide-lipid interactions that might be related to the target cell specificities already demonstrated. We refer to selectivity as selective interaction or specificity that is usually associated to binding affinity, to the regulatory role of the electrostatic interactions and of the peptide to lipid molar ratio, which vary with the bilayer composition, as already demonstrated by works of H. W. Huang group (Huang 2000; Chen et al. 2003; Lee et al. 2005). Thus the mechanism of action of Polybia-MP1 was investigated in dye leakage experiments, from electrically neutral and charged vesicles; its secondary structure was studied through circular dichroism (CD) spectroscopy, and the molecular origin of selectivity was prospected, in comparison with MP-X (INWKGIAAMAKKLL-NH_2), with the help of molecular dynamic simulations (MD).

The selectivity in the mechanism of action of Polybia-MP1 is expressed through the different concentrations of peptide and lipids (P/L) needed to reach the point of starting the cooperative leakage process, which depends on the bilayer composition, and follows different rates of leakage. At this P/L threshold value, just before the peptide forms multiple pores (or defects), with intense leakage, we found out that the apparent average pore number differentiates anionic from zwitterionic vesicles, and suggests that the formation of pores and their constitution should be similar, depending on the ionic character of phospholipids in the bilayer. We also found that the selective way of action of Polybia-MP1 in comparison to other mastoparans can be associated to its lower net charge and to a low hydrophobicity, as proposed in the theoretical model by Taheri-Araghi and Ha (2007). Molecular dynamics simulations also showed that there are structural reasons that differentiate peptides with and without selectivity in their way of action. Particularly, we emphasize the distribution of positively and negatively charged residues, as well as polar residues, which favor the electrostatic equilibrium and would exert a smaller influence on the bilayer organization.

Materials and methods

Chemicals

Sigma-Aldrich Co. (St.Louis, MO, USA) has supplied all lipids and carboxyfluorescein (CF). Other chemicals were of high quality analytical grade. Buffers: Tris/HCl 10 mM, 1 mM Na_2EDTA, pH 7.5, either containing 25 mM CF (vesicles formation) or 150 mM NaCl for the leakage experiments and Tris/H_3BO_3 5 mM, 150 mM NaF, 0.5 mM Na_2EDTA, pH 7.5 for CD and fluorescence spectroscopy experiments.

Peptide synthesis, purification and mass spectrometry analyses

Polybia-MP1 was synthesized, as described by Souza et al. (2005) by step-wise manual solid-phase synthesis using N-9-fluorophenylmethoxycarbonyl (Fmoc) strategy. The crude product was purified by reverse-phase HPLC and the homogeneity and sequence was accessed by analytical HPLC and mass spectrometry (ESI-MS).

Samples were analyzed on a triple quadrupole mass spectrometer, model QUATTRO II, equipped with a standard electrospray (ESI) probe (Micromass, Altrinchan),

adjusted to ca. 250 µl/min. The source temperature was maintained at 80°C and the needle voltage at 3.6 kV, applying a drying gas flow (nitrogen) of 200 L/h and a nebulizer gas flow of 20 L/h. The mass spectrometer was calibrated with intact horse heart myoglobin and its typical cone voltage-induced fragments. The molecular masses were determined by ES-MSI, adjusting the mass spectrometer to give a peak width at half-height of 1 mass unit and the cone sample to skimmer lens voltage, controlling the ion transfer to mass analyzer, was set to 38 V. About 50 pmol (10 µl) of each sample was injected into electrospray transport solvent. The ESI spectra were obtained in the multichannel acquisition mode; the mass spectrometer data acquisition and treatment system was equipped with MassLynx and Transform software for handling spectra.

Vesicle preparation

Large unilamellar vesicles (LUV) for dye leakage experiments and small unilamellar vesicles (SUV) for CD and fluorescence spectroscopy were prepared according to general procedures from the literature (Allende and McIntosh 2003) with modifications (dos Santos Cabrera et al. 2004). Lipids in chloroform have been evaporated under N_2 flow, rendering homogeneous films on the walls of test tubes that have been further dried under vacuum for at least 3 h. These films were hydrated with respective buffers for dye leakage experiments or CD and fluorescence spectroscopy to reach a final lipid concentration around 10 mM, as a standard procedure. Afterward, the actual lipid concentration was confirmed by phosphorus analysis (Rouser et al. 1970). After hydration, the suspensions were thoroughly vortex mixed at room temperature. LUV were obtained after 5-min sonication and SUV after a 50-min sonication (or until clear) with a tip sonicator in an ice/water bath, under N_2 flow; titanium debris was removed by centrifugation. LUV have been submitted to 11 extrusions through two-stacked 200 nm polycarbonate membranes, at room temperature, using an Avanti mini-extruder, and filtered through a Sephadex G25 M gel column (Amercham Pharmacia, Uppsala, Sweden) to separate dye-entrapped LUV from free dye. They were used within 48 h of preparation and SUV within 24 h, as obtained after Ti debris removal. Both were kept under refrigeration and protected from light.

Zwitterionic and negatively charged lipid mixtures were prepared and thoroughly homogenized at the following molar ratios: pure L-α-phosphatidylcholine (PC) and PC plus cholesterol (named PCC) at 80:20, and mixtures made of PC and either L-α-phosphatidyl-DL-glycerol (PG) or cardiolipin (CL), as PC:PG at 70:30 (named PCPG 7030), or at 40:60 (PCPG 4060), PC:CL at 70:30 (PCCL 7030).

Dye leakage

To complete a final volume of 1.2 ml, an aliquot of fresh LUV suspension was injected into a 1-cm quartz cell, containing magnetically stirred peptide solutions in Tris/HCl buffer at different concentrations, ranging from 1.0 to 20 µM, according to the permeabilizing efficiency, to reach around 100% leakage within 20 to 30 min of contact time. With an ISS PC1 spectrofluorometer (Urbana Champaign, IL, USA), CF release from vesicles was monitored at 520 nm, 0.5 nm slit width, (excited at 490 nm, 1 nm slit width) by measuring the decrease in self-quenching at 25°C. Percentage of dye leakage was determined after regular time intervals, and calculated with the equation:

$$\text{Percentage of leakage} = 100 \times (F - F_0)/(F_{100} - F_0) \quad (1)$$

where F is the observed fluorescence intensity, F_0 and F_{100} correspond, respectively, to the fluorescence intensities in the absence of peptides and to 100% leakage, as determined by the addition of 20 µl of 10% Triton X-100 solution. F_{100} has been corrected for the corresponding dilution factor. The observed release of CF from vesicles is described by a single exponential function as proposed by Schwarz and Robert (1990) and recently reviewed and expanded by Andersson et al. (2007). However, in the present study the leakage time course curves could only be fitted for all kinds of vesicles and peptide concentrations tested, with correlation factors above 0.97, most of them above 0.99, using the relationship

$$\text{Leaked fraction} = L_{\max} - L_i{}^{*}\exp(-kt), \quad (2)$$

where $L_{\max}$ represents the maximum (steady state) leakage, or the fraction of CF released at the rate k, L_i is a constant that accounts for the leakage that occurs immediately at vesicle addition, i.e. when at $t \approx 0$, $L \neq 0$, t is the time elapsed after the addition of vesicles and k is a constant measuring the rate of leakage. This empirical exponential model is similar to that proposed by Ladokhin et al. (1997). The constant k was determined by verifying that

$$\ln((E(t) - 1 + L_{\max})/L_i) = -kt \quad (3)$$

fits to a straight line in each experiment, with

$$E(t) = 1 - \text{Leaked fraction}. \quad (4)$$

The induced flow-rate of leakage of CF molecules, τ, was obtained from

$$\tau = 1/k. \quad (5)$$

The efflux function $E(t)$ was also employed to directly obtain the apparent average pore number, as

$$p^{*}(t) = -\ln E(t), \quad (6)$$

which is based on the assumption that vesicles are homogeneous in size (Schwarz and Robert 1990).

Circular dichroism measurements

The CD spectra were obtained at 20 μM peptide concentration in different environments: Tris/H_3BO_3 buffer, trifluoroethanol (TFE)/water mixture (40% v/v), sodium dodecyl sulfate solution (8 mM), or in the presence of zwitterionic PC and PCC SUV, and in anionic PCPG 7030, PCPG 4060 and PCCL 7030 SUV at 100 or 200 μM concentration. Buffer, peptide and lipid concentrations have been chosen to minimize noise-to-signal ratio and light scattering, and to provide similar conditions to the dye leakage experiments. CD spectra were recorded from 260 to 190 nm with a Jasco-710 spectropolarimeter (JASCO International Co. Ltd., Tokyo, Japan), which was routinely calibrated at 290.5 nm using d-10-camphorsulfonic acid solution. Spectra have been acquired at 25°C using 0.5 cm path length cell, averaged over six scans, at a scan speed of 20 nm/min, bandwidth of 1.0 nm, 0.5 s response and 0.1 nm resolution. Following baseline correction, the observed ellipticity, θ (mdeg) was converted to mean residue ellipticity [Θ] (deg cm^2/dmol), using the relationship

$$[\Theta] = 100\theta/(l\,c\,n), \tag{7}$$

where "l" is the path length in centimeters, "c" is peptide milimolar concentration, and "n" the number of peptide residues. Assuming a two-state model, the observed mean residue ellipticity at 222 nm ($\Theta^{obs}{}_{222}$) was converted into α-helix fraction (f_H) using the method proposed by Rohl and Baldwin (1998) and previously described (Konno et al. 2001).

Fluorescence spectroscopy

Tryptophan emission fluorescence spectra were collected using a quartz cell with 1 cm path length, at 25°C. The spectra were recorded from 300 to 450 nm with Trp residue excitation set at 280 nm, with an increment of 1 nm, averaging in five scans. Excitation and emission bandwidth were set at 1 and at 0.5 nm, respectively. In these experiments samples were the same used to record the CD spectra, after 1 h of sample preparation. The position of the maxima did not change even after 24 h. Correction for scattering was carried out by subtracting spectra obtained for each vesicle composition from blank of peptide samples. Blue shifts ($\Delta\lambda_{max}$) were calculated as the differences in wavelength of the maxima in emission spectra of the peptide acquired in the presence or absence of membrane mimetics; the variation of Trp fluorescence intensity (F/F_0) was calculated as the intensity ratio between the maxima of the same spectra. Standard deviation for the blue shift was 1 nm.

MD simulations

The MD simulations were performed in TFE/water ($\sim$30% v/v) mixture for peptides Polybia-MP1 in comparison to MP-X. Systems were made up, respectively, by 201 or 199 TFE molecules, 1893 water molecules and 2 or 4 chlorine (Cl^-) counterions, which neutralize the net charge of each peptide. In both cases the N-termini were treated as a positively charged group (NH_3^+) and amidated C-terminus. Force field in MD calculations is GROMOS 96 (van Gunsteren et al. 1996); model SPC (Simple Point Charge; Berendsen et al. 1981) was used for water, and for TFE molecules the model proposed by Fioroni et al. (2000). System optimization was carried out in 8,000 steps conjugate gradient and a steepest descent cycle was performed every 500 steps. Position restriction dynamics, for solvent and ions relaxation ran for 1 ns, with a 2 fs-time step for the integration of the equations of motion. Afterward, constraints have been removed and the systems underwent 20 ns MD simulations. Periodic boundary conditions have been imposed in the systems simulations with a cutoff radius of 1.4 nm. The LINCS (Hess et al. 1997) algorithm was used to constraint all bond lengths and SETTLE (Miyamoto and Kollman 1992) to constraint water geometry. Simulations ran in the canonical ensemble (n, P, T) 300 K and 1 atm. Temperature and pressure were modulated using coupling techniques (Berendsen et al. 1984) with coupling and isothermal compressibility constants of 0.01 ps (solvent and peptide) and 6.5×10^{-5} bar^{-1}, respectively. Long-range electrostatic interactions were treated using PME ("Particle Mesh Ewald"; Cheatham et al. 1995) method. For Lennard–Jones interactions the cutoff radius was 1.4 nm. The atomic positions were recorded every 10 ps throughout each trajectory. MD calculations and trajectory analysis were carried out using the facilities of the GROMACS package (Lindahal et al. 2001).

The strategy for the MD studies of Polybia-MP1 in TFE/water mixture was to use one of the 14 structures determined from NMR experiments of MP-X bound to G-protein (Kusunoki et al.1998), where the different residues in Polybia-MP1 have been substituted accordingly. An equivalent simulation was run for the MP-X structure.

Results

Dye leakage

Permeabilization of anionic and zwitterionic bilayers is often correlated either with antimicrobial or hemolytic activity of peptides, since high negative charge density is characteristic of the outer leaflet of bacterial membranes, whereas in mammalian membranes zwitterionic lipids

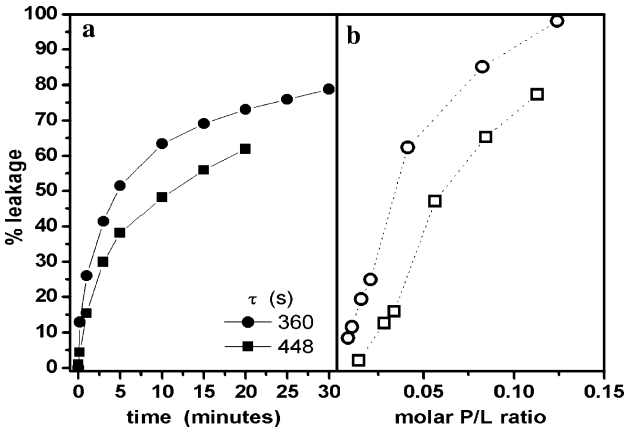

Fig. 1 Zwitterionic bilayer permeabilization induced by Polybia-MP1, at 5 μM, 25°C. **a** Leakage kinetics in PC (*circles*) and PCC 8020 (*squares*) LUV. P/L is 0.0413 and 0.0565, respectively. **b** Dose–response curves after 10 min vesicle addition (*open symbols*, same legend), as a function of peptide to lipid molar ratio (P/L). Threshold P/L values are 0.015 for PC and 0.032 for PCC vesicles

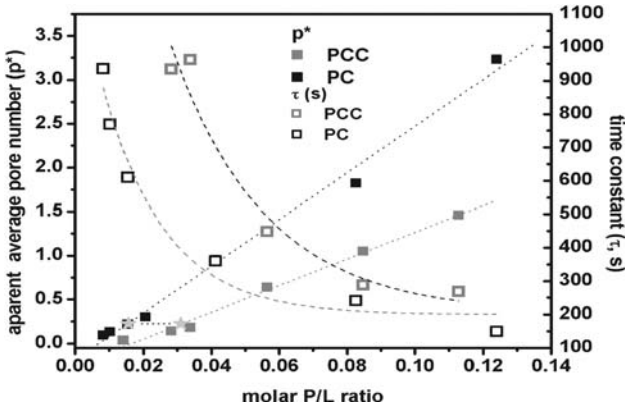

Fig. 2 Apparent average pore number function (p^*, Eq. 6, *closed symbols*) and time constant (τ, Eq. 5, *open symbols*) plots as a function of the P/L molar ratio for PC (*black*) and PCC 8020 vesicles (*gray*). Stars (*gray*) indicate threshold P/L concentration

predominate; moreover, cholesterol is characteristic of eukaryotic membranes and is essentially absent in the prokaryotic, as well as PG and CL are highly frequent in the latter and absent in the former (Yeaman and Yount 2003; Lohner and Prenner 1999). To mimic these interactions these lipids were used to modify the characteristics of vesicles, originally made of PC, to the following compositions: zwitterionic PC and PCC 80:20 vesicles (Figs. 1, 2) and in anionic PCPG 70:30 and PCCL 7030 (Figs. 3, 4).

Figures 1a and 3a present typical time course leakage curves whose induced flow-rate constants, τ, are shown as inserts for comparison; τ values were obtained applying equations 2 and 5 to each leakage curve (these examples were obtained at P/L of 0.0413 and 0.0565, respectively, with PC or PCC vesicles). The release of CF entrapped in LUV due to the lytic activity of Polybia-MP1 has been

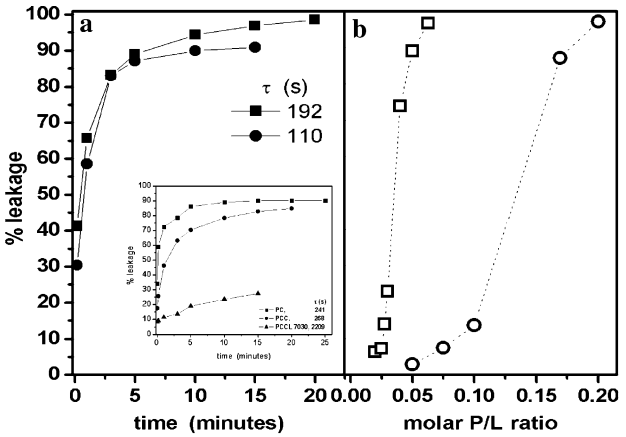

Fig. 3 Anionic bilayer permeabilization induced by Polybia-MP1, 25°C. **a** Leakage kinetics at 5 μM and at 17 μM, respectively, in PCPG 7030 (*squares*) and PCCL 7030 (*circles*) LUV, corresponding to P/L 0.05 and 0.169. The *inserted plot* compares the influence of cholesterol and cardiolipin on the leakage kinectics of Polybia-MP1 at 10 μM. **b** Dose–response curves after 5 min of vesicle addition (*open symbols*, same legend), as a function of P/L ratio. Threshold P/L values are 0.025 for PCPG 7030 and 0.10 for PCCL vesicles

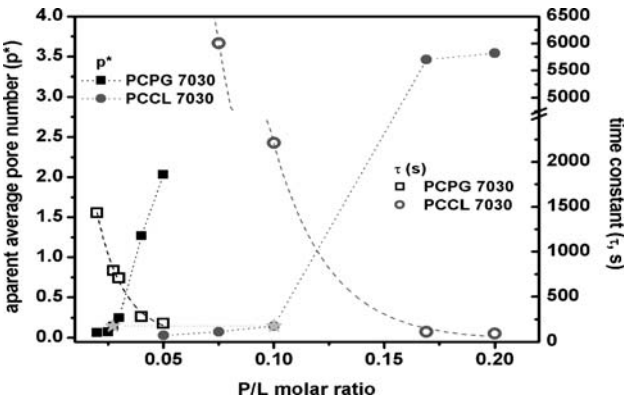

Fig. 4 Apparent average pore number function (p^*, Eq. 6, *closed symbols*) and time constant (τ, Eq. 5, *open symbols*) plots as a function of the P/L molar ratio for PCPG 7030 (*black*) and PCCL 7030 (*gray*) LUV. Stars (*gray*) indicate threshold P/L concentration. (A break in τ axis has been used for the sake of clarity)

found to depend on the lipid composition of vesicles and on the peptide concentration, showing sigmoid dose-response curves. In these curves (Figs. 1b, 3b), at low peptide-to-lipid ratios, the peptide causes low or hardly detectable leakage of the internal dye; at a P/L above a threshold value, the peptide causes intense leakage. This suggests that a sequence of effects occurs depending on peptide concentration: at lower concentrations leakage is slow and does not reach 40% of total content, even after long contact time; at concentrations near the threshold the process is faster and reaching higher (around 80%), but not total leakage; at higher concentrations leakage reaches completeness (or almost) in few minutes. A similar sequence of

steps has been recently described for the peptide surfactin (Heerklotz and Seelig 2007).

In zwitterionic vesicles the presence of cholesterol increases τ, decreases L_{max}, the maximum leakage, moves the threshold concentration upward, from 0.015 in PC to 0.032 in PCC, and reduces cooperativity. Comparative leakage curves obtained for melittin in PC and 1:1 PC/cholesterol show similar behavior, with greater influence of the cholesterol content (Allende et al. 2005). Cholesterol increases the compressibility modulus and the line tension at the pore edge required to rupture the vesicle and decreases the area per phospholipid molecule in bilayers, depending on its concentration (Needham and Nunn 1990). Other effects related to the presence of cholesterol in bilayers or monolayers, at lower concentrations (10%) have been reported, such as the reduction of Temporins B and L penetration into the lipid films (Zhao et al. 2002). Likewise, Fig. 1b shows an attenuation effect due to the presence of cholesterol.

Figure 2 shows that the flow-rate constant, τ, which is related to the rate of pore formation (Schwarz and Robert 1990), exponentially decays with P/L molar ratio, while the apparent average pore number (p^*), obtained from applying Eqs. 4 and 6 to the leakage kinetics curves, increases linearly, indicating that a mechanism of pore inactivation should be at play. Figure 2 (gray stars) also shows that at the respective threshold P/L concentrations, the average apparent pore number is approximately the same for both zwitterionic vesicles, around 0.23. It should be noted that the proper pore number function (Schwarz and Robert 1990) has been calculated for the vesicles of this study and it is coincident with $p^*(t)$ for the lower P/L molar ratios, around the threshold P/L ratio, implying that the size distribution of these vesicles is fairly homogeneous, as expected from extruded LUV.

The influence of anionic lipids, characteristic of the outer layer of prokaryotic membranes is depicted in Fig. 3a, b. They have an opposite effect in PC vesicles in relation to the influence of cholesterol; this means that anionic lipids reduce τ, above the threshold P/L value, increase L_{max}, and enhance cooperativity. However, they increase the threshold P/L molar ratio to 0.025 in PCPG 7030 and to 0.10 in PCCL 7030 vesicles. CL is a dimeric form of PG, with four acyl-chains and two phosphates at the head group region that imposes negative curvature strain to bilayers (Matsuzaki et al. 1998), while in PG the cross-sectional area of the head group matches the cross-sectional area of the acyl chains (Lohner and Prenner 1999). According to Haines and Dencher (2002), at pH below 8.0, CL has a single negative charge on a small head group that would confer about the same charge density as in PCPG 7030, providing equivalent electrostatic components in peptide binding to bilayers. The kinetics of anionic vesicles permeabilization shown in Fig. 3a was obtained at 5 and 17 μM (corresponding to P/L = 0.05 and 0.169) of Polybia-MP1, respectively, in PCPG and PCCL 7030, to illustrate the lytic activity of the peptide above the threshold P/L value and at equivalent flow-rates (τ). Matsuzaki et al. (1998), working with magainin, also observed a dramatic increase in P/L values necessary to induce calcein release from cardiolipin (ex-*Escherichia coli*) vesicles in comparison with egg-PG vesicles. Lee et al. (2005) demonstrated that lipids with smaller head groups or with a greater acyl chain-head group differential have more room to accommodate peptide adsorption, increasing the threshold P/L ratio. The insert in Fig. 3a directly compares the influence of cholesterol and cardiolipin in the lytic activity of Polybia-MP1 at 10 μM and shows the respective τ constants. Although cationic peptides usually show stronger preference for anionic vesicles, the lytic activity of Polybia-MP1 is significantly influenced by the negative curvature strain imposed by CL that attenuates the positive curvature strain imposed by the peptide (Lohner and Prenner 1999), hampering its pore-forming ability.

For the anionic lipids it has also been observed that the flow-rate constant, τ, exponentially decays with P/L molar ratio, while the apparent average pore number (p^*) increases in a sigmoid-fitted fashion (Fig. 4), emphasizing the cooperativity in the mechanism of pore formation, particularly evident in PCCL 7030 bilayer. At the respective threshold P/L concentrations (gray stars), the average apparent pore number is approximately the same for both anionic vesicles, 0.15. Dose–response curves of MP-X in PCPG 7030 vesicles show a similar profile, but threshold P/L ratio is around 0.01 (Matsuzaki et al. 1996), while for Polybia-MP1 it is 0.025.

CD spectroscopy

The CD spectra of Polybia-MP1 at 20 μM, in water or Tris buffer, show a band at 203 nm, characteristic of unordered structures. In membrane mimetic environments such as 40% TFE/water mixture, or 8 mM SDS solution or in vesicles, as zwitterionic (PC, PCC) and anionic (PCPG 7030, PCPG 4060, PCCL 7030), spectra present typical bands at 206–208 and 222 nm (S1). Ellipticity increases in the order PCC < PC < PCPG 7030 ≅ PCPG 4060 = 40% TFE < PCCL 7030, suggesting that bilayer composition other than charge density seems to be the determining parameter. Except for PCCL 7030, an isodichroic point at 204 nm has been detected among PC, PCC and all PCPG vesicles. It indicates that in these environments chains are mainly present in two states, helix and random coil (Rohl and Baldwin 1998) and that the interactions of Polybia-MP1 with these vesicles are of the same nature, but with different binding affinities. CD spectra presented by

Chuang et al. (1996) and McDowell et al. (1985), respectively, for mastoparans MP-B in 40% TFE and MP-X in 70% TFE, also show an isodichroic point around 200 nm. A complementary evaluation of the secondary structure of Polybia-MP1 in anionic vesicles was carried out by fitting of spectra with CDPro programs (CONTIN, SMP56); they indicated a slightly more ordered structure for the peptide in PCCL 7030 vesicles than in PCPG 7030, with helical contents ranging from 47 to 67%.

Table 1 presents the amino acid sequences of Polybia-MP1 in comparison to MP-B and MP-X and other structural similarities among these peptides. There is a pronounced structural similarity between Polybia-MP1 and MP-B, in relation to the position of charged and polar residues, intercalated by apolar residues of equivalent size. Despite a marked difference in the net charge value (Q), both peptides present negative mean hydrophobicity (H) and a similar mean hydrophobic moment (μ), calculated according to consensus scale of Eisenberg et al. (1984). Moreover, the α-helical content of Polybia-MP1 in PCPG 7030 is very similar to that observed for MP-B at the same L/P ratios by Park et al. (1995).

Fluorescence spectroscopy

Polybia-MP1 at 20 μM in Tris/H_3BO_3 buffer has a fluorescence emission maximum at 351 nm (S2), compatible with those of Trp in a polar environment (Ladokhin et al. 2000). Upon the addition of vesicles at 100 μM, Trp spectral changes were observed, indicating the differences in the interaction of the peptide with zwitterionic or anionic vesicles. In zwitterionic vesicles emission intensity was attenuated and blue shifts were smaller, in contrast with anionic vesicles, in which emission intensity and blue shifts increased. These fluorescence changes are characteristics of binding and burial of Trp residues in a more hydrophobic environment. In PCC 80:20 blue shift and fluorescence intensity were the smallest, whereas in PCCL 7030 the maximum intensity was observed, with blue shifts being very similar among the anionic vesicles, and ranging from 26 to 29 nm. Other peptide/lipid ratios were tested and Fig. 5 shows a correlation picture between CD and Trp fluorescence measurements; data obtained in 40% TFE and 8 mM SDS are shown for comparison. Although SUV are not the most preferred models for fluorescence experiments (Ladokhin et al. 2000), they are required for CD spectra recording and were used as a means to correlate conformational transitions and Trp environment. Even though, some spectra of Polybia-MP1 in LUV have been independently acquired, at the same condition as with SUV, and no change in the position of maxima has been detected.

In zwitterionic vesicles, the lower helical content ranges from 20 to 28.5% and correlates with smaller blue shifts ranging from 11 to 20 nm. Small variations on ellipticity and blue shifts with the increase on peptide to lipid ratio are within the s.d. of the experiments (±0.02 for CD and ±1 nm for fluorescence); although, as a general tendency, they could indicate that the burial of the Trp residue occurs at the cost of small conformational changes. In PCC vesicles, a lower peptide to lipid ratio was tested (3/100 μM), around the P/L threshold concentration observed in the dye leakage experiments. The position of the maxima, around 340 nm, is compatible with the interpretation given by Ladokhin et al. (2000) for an aggregate in which some Trp residues are exposed and some are buried; this might also account for the fact that blue shifts are smaller at higher peptide to lipid ratios, at which the fraction of exposed molecules would be higher than that of the buried.

The α-helix fraction of Polybia-MP1 is considerably higher in PCCL vesicles, which could be owed either to a higher fraction of bound peptide or to differences in the conformation of the bound peptide. Among anionic vesicles blue shifts do not vary and emission fluorescence increases upto maximum 12% with the increase in lipid contents, suggesting that the fraction of bound peptide is similar under these conditions. These results show also that the increase in charge density represented by PCPG 4060 vesicles does not affect significantly the peptide binding to the bilayer. Other environments like the micellar SDS solution induced the highest blue shift, $\Delta\lambda_{max} = 35$ nm; these micelles have a high negative charge density and Trp fluorescence depends on the polarity and rigidity of local environment (Ladokhin et al. 2000).

The blue shifts observed in the spectra with PC and PCPG 7030 vesicles are compatible with the changes observed in the fluorescence spectra of MP-X, which also has a Trp at position 3; they were observed at an equivalent ratio in PCPG 7030 and at much lower peptide to lipid ratios, 3/100, in PC (Matsuzaki et al. 1996). Comparing with MP-B, which has a Trp9 residue, equivalent blue shifts were also observed in much smaller peptide to lipid ratios (Park et al. 1995). Both, MP-X and MP-B, show a decrease in the fluorescence emission at the lowest PC concentration and a significant increase in anionic vesicles.

Molecular dynamic simulations and trajectory analysis

As shown by CD spectroscopy, MD simulations also indicate that Polybia-MP1 present amphipathic α-helical structure in TFE/water mixtures.

The average RMSD value obtained throughout the simulation is 0.025 nm for MP-X and Polybia-MP1 indicating that their conformations are close to that of the ideal helix in TFE/water mixture (S3). Although both sequences differ mainly in relation to residues 8 to 14, they fluctuate

Table 1 Primary structures and structural characteristics of Polybia MP1 in comparison with MP-B and MP-X

MP1	Ile-Asp-Trp-Lys-Lys-Leu-Leu-Asp-Ala-Ala-Lys-Gln-Ile-Leu-NH_2
MP-B	Leu-Lys-Leu-Lys-Ser-Ile-Val-Ser-Trp-Ala-Lys-Lys-Val-Leu-NH_2
MP-X	Ile-Asn-Trp-Lys-Gly-Ile-Ala-Ala-Met-Ala-Lys-Lys-Leu-Leu-NH_2

					f_H			
	Q[a]	H	Φ[b]	μ	TFE[c]	SDS[d]	PCPG 7030	PC
MP1	+2	−0.108	90°	0.297	0.410	0.423	0.362[e]	0.266[e]
MP-B	+5	−0.064	136°[f]	0.270	0.497[f]	–	0.366[g]	0.165[g]
MP-X	+4	0.009	90°	0.209	0.61[h]	–	–	0.61[i]

Charged and polar residues are shown in gray. Net charge (Q), hydrophobicity (H), polar angle (Φ), hydrophobic moment (μ), and α-helix fraction (fH) at 20 μM, in different environments

[a] Includes an extra charge due to the amidated C-terminus

[b] Polar angle according to MD simulation

[c] 40% TFE

[d] 8.0 mM SDS

[e] L/P ratio = 10

[f] Calculated from Chuang et al. (1996)

[g] Calculated from Park et al. (1995), at L/P ratio = 10

[h] Calculated from McDowell et al. (1985)

[i] Schwarz and Blochmann 1993

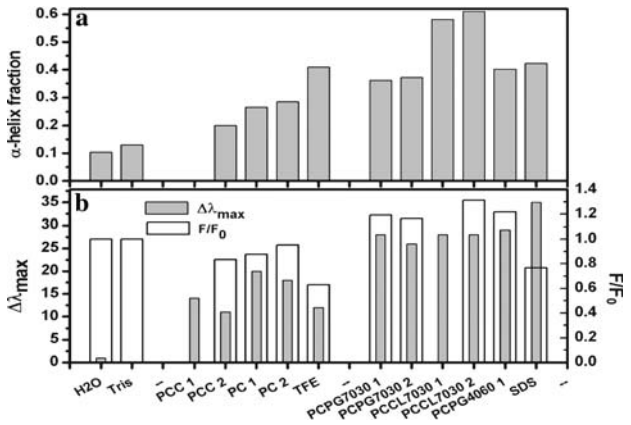

Fig. 5 CD and Trp fluorescence spectroscopy data correlation plot for Polybia-MP1 at 20 μM. a α-Helix fraction in different environments, at 25°C. **b** Trp fluorescence blue shifts ($\Delta\lambda_{max}$) and variation of Trp fluorescence intensity (F/F_0) at the same environments. Tris = Tris buffer pH 7.5; PCC1 and PCC2 SUV for P/L ratios of 0.03 and 0.2, respectively; remaining SUV P/L ratios are 0.1 (indicated 1) and 0.2 (indicated 2); TFE at 40% and SDS at 8 mM. (F/F_0 for PCC1 and PCCL 70301 are not available; blue shifts have been obtained in independent experiments)

according to the same pattern. Table 2 shows the lifetime of all hydrogen bonds of type $i, i + 4$; the residues I1 and N2 in MP-X are neither structured in membrane environments (Wakamatsu et al. 1992) nor in TFE/water mixtures. Hydrogen bonds between residues 1 and 5 do not form during the simulations: for MP-X this confirms the unfolding of residue 1, and suggests that Polybia-MP1 also presents this structural characteristic, found in other mastoparans (Hori et al. 2001). The hydrogen bond between O in residue 2 and N in residue 6 is more stable in Polybia-MP1 due to the presence of another hydrogen bond between the charged group of D2 and N of the backbone in K5. In MP-X the second residue is not charged; actually it is a polar N2, whose O in the side chain resonates between N of the backbone in K4 and G5 (Table 2).

Judging from the lifetimes obtained, the hydrogen bonds between residues 8–12 and 9–13 in Polybia-MP1 are less stable than in MP-X and this can be explained analyzing the charge distribution and the respective solvation profile of this region. Figure 6 represents the solvent distribution around the peptide helix, focusing on the region around residue Asp8 and showing the increased number of water molecules near the backbone, which are not seen with MP-X. Using GROMACS package (Lindahal et al. 2001) a solvation analysis has also been carried out (data not shown) and it showed that the difference in the solvation profile is a consequence of the charge distribution: MP-X has+4 positive charges (3 Lys and the amidated C-terminus) while Polybia-MP-I has +2 net charge (3 Lys, the amidated C-terminus and 2 negative charges, Asp2 and Asp8). Compared to Lys, Asp side chain is considerably short and its COO^- group interacts favorably with water dipoles, driving more water molecules to its surrounds, nearer the backbone.

Table 2 % Permanence time of the hydrogen bonds between side chains of residues Asn 2 and Asp 2 with the backbone of peptides MP-X and Polybia MP1, respectively, and between hydrogen bonds of type i, $i + 4$ within the main chain, for both peptides (in relation to the total simulation time)

	n, n + 2[a]	n, n + 3[a]	i, $i + 4$ Hydrogen bonds								
	2–4	2–5	2–6	3–7	4–8	5–9	6–10	7–11	8–12	9–13	10–14
MPX	31.2	59	70	96	95	95	96.1	93.1	90	89	80
MP1	–	90	94	97.6	95	96.3	98	94.5	77	76	77

[a] O (side chain with N backbone)

Considering the electrostatic interactions that might be playing, an average structure of the total simulation time of Polybia-MP1 has been obtained (Fig. 7a, b). The analysis of the distance between charged atoms in Fig. 7a showed that O^- of Asp 2 is around 0.75 nm far from NH_3^+ (N-terminal), 0.72 nm far from NH_3^+ of Lys 4 and 0.6 nm far from NH_3^+ of Lys 5 and is part of the hydrogen bond with N of Lys 5 backbone during 90% of the simulation time (Table 2). We observed that an electrostatic equilibrium appears relating Asp 2 and groups NH_3^+ of N-terminal and Lys 4 and Lys 5, at the point where the electric field, due to the positive charges, is minimized. This situation favors that the hydrogen bond, which is part of the equilibrium, as well as this charge distribution, is kept stable throughout the simulation (Table 2). Figure 7b shows the charge equilibrium around O^- of Asp 8: this negative charge is kept closer to NH_3^+ of Lys 11 and of NH_2 of Gln 12 (polar group). The analysis of the distances between these charged groups showed that they fluctuate around 0.4 nm, presenting a certain complementary positioning in relation to the distance between O^- and NH_3^+ of Lys 11. This equilibrium encompasses also NH_3^+ of Lys 5 and NH_3^+ of Lys 4. The three cationic and the polar groups form approximately a tetrahedron in which the negative charge, O^- of Asp 8, is the apical point (Fig. 7b), also minimizing the electrical field of these charges. This spatial distribution of charges partially counterbalances the smaller permanence time of the hydrogen bonds, mainly those including residues 8 to 14, as demonstrated in Table 2.

Discussion

Peptide-induced membrane permeabilization is part of the mechanism of action of Polybia-MP1 and depends importantly on the lipid composition of the bilayer and the peptide structure. The lytic activity of Polybia-MP1 on zwitterionic and anionic vesicles is characterized by different threshold P/L molar ratios, different rates of leakage, and by sigmoidal concentration dependence. Preferential interaction with anionic vesicles is denoted by lower flow-rate constants (τ), above the threshold P/L concentration and higher cooperativity, although the mechanism of dye release is similar to that observed in zwitterionic vesicles. Polybia-MP1 destabilizes and promotes leaking in vesicles at concentrations of the same order as those presenting antimicrobial activity (Souza et al. 2005).

In zwitterionic bilayers containing cholesterol, the attenuation of the lytic activity and the increase in τ, in relation to PC vesicles, are well correlated with the stabilization effect of cholesterol in eukaryotic membranes that inhibits the hemolytic activity (Zasloff 2002), and with

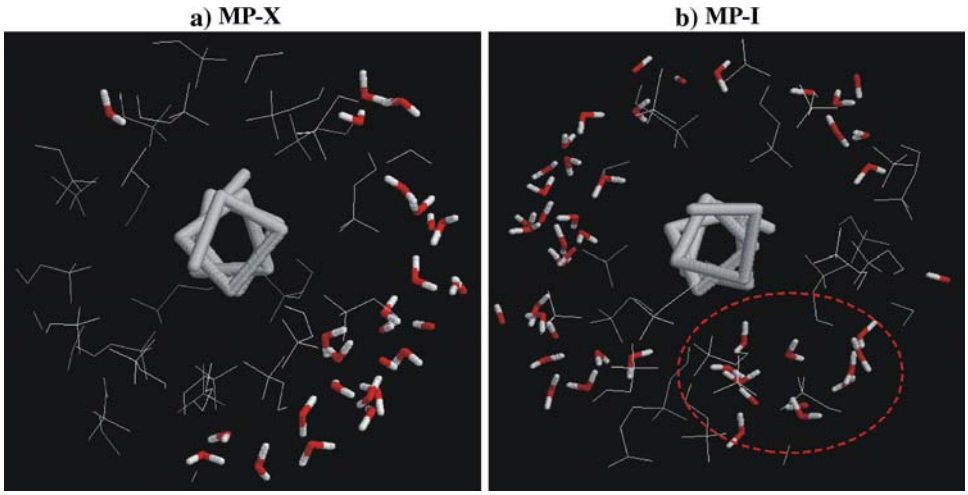

Fig. 6 Solvation profile around the peptide helix (*thick*, *gray* rod-like), focusing on region around residue 8. a MP-X, **b** Polybia-MP1, showing the increased number of water molecules near the backbone at Asp8. TFE molecules are shown as *thin*, *gray* sticks and water molecules as *red* and *white* rods

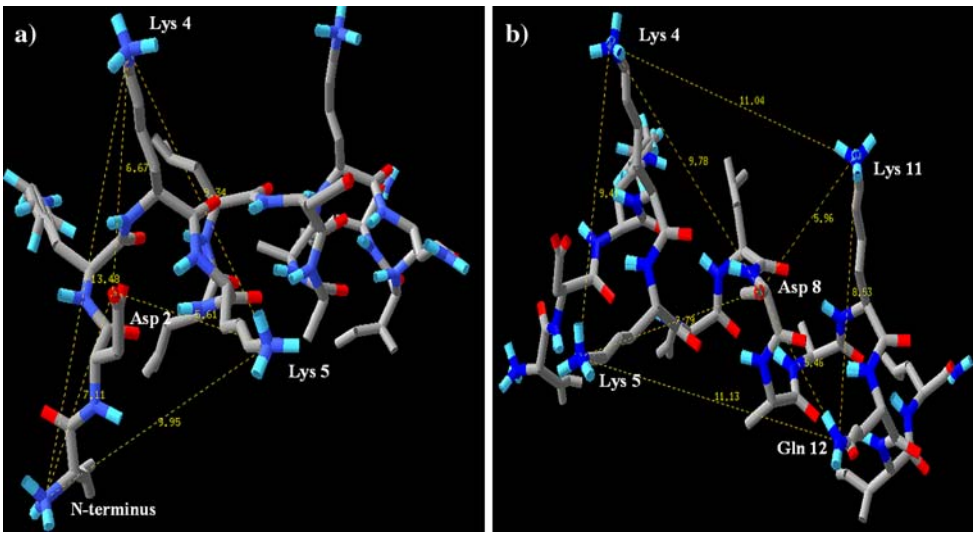

Fig. 7 Polybia-MP1 average projection obtained in the simulation run. **a** Distances between positive charges (N-terminus, Lys 4 and Lys 5) and the negative Asp 2. **b** Distances between positive charges, including polar residues (Lys 4, Lys 5, Lys 11 and Gln 12) and the negative Asp 8. *Dotted lines* indicate distances (in Å) between charged or polar groups. N atoms in *blue*, H atoms bound to electronegative atoms in *light blue*, C atoms in *gray* and O atoms in *red*

the increase in the compressibility and bending modulii of the bilayer hampering the lytic activity, as also demonstrated for melittin (Allende et al. 2005). Needham and Nunn (1990) showed that with SOPC vesicles, increasing cholesterol contents in bilayers increases exponentially the compressibility modulus. Cholesterol can also undergo a fast flip to the inner leaflet compensating the asymmetric expansion due to peptide binding to the outer leaflet (Lange et al. 1981). The smaller blue-shifts in the Trp emission spectra and the lower helicity observed with PC and PCC vesicles confirm the shallower interaction of Polybia-MP1 with the zwitterionic than with the anionic vesicles (Fig. 5). However, this preference alone does not explain its selectivity. MP-X also showed lower affinity with PC vesicles than with PCPG 7030, with smaller blue-shifts than Polybia-MP1 (Matsuzaki et al. 1996), although being a hemolytic peptide. A Polybia-MP1 analog with an Asn2 instead of Asp2 shows similar blue-shifts in PC vesicles (data not shown), but this modification turned the peptide hemolytic (Souza 2007).

The selectivity of cationic Polybia-MP1 for the anionic vesicles most probably derives from electrostatic interactions, which are evidenced in the higher helicity observed in the corresponding spectra, and also found with other mastoparan peptides (Park et al. 1995; dos Santos Cabrera et al. 2004). CD spectra in PCCL 7030 vesicles present an interestingly higher helicity that can not be attributed to differences in the binding process, when compared to PCPG 7030 or PCPG 4060 vesicles, since the penetration depth of the Trp residue shows hardly any difference among the anionic vesicles (Fig. 5). Considering that the lipid head groups are the same and that higher charge density, represented by PCPG 4060 vesicles, also did not increase helicity, other characteristics of the bilayer such as the curvature and hydration should be playing a role. Matsuzaki et al. (1998) observed that magainin presents the same molar ellipticity in PCPG 1:2 and 100% CL (ex- *E. coli*) vesicles, which have different curvature strains. Since helicity depends on the absence of competition between intramolecular H-bonds and the solvent, it is reasonable to suggest that there should be less room for the aqueous solvent and more favorable conditions to protect the intramolecular H-bonds in our PCCL 7030 vesicles (made of CL ex-bovine heart) than in PCPG 7030. Moreover, on binding, Polybia-MP1 should be a better releaser of water molecules from the head group region, according to the mechanism proposed by Lee et al. (2005). A more hydrophobic environment can also explain the greater blue-shifts observed with Polybia-MP1 in relation to MP-X (Matsuzaki et al. 1996).

The lytic activity of Polybia-MP1 on PCPG and PCCL 7030 vesicles shows a marked susceptibility of the PG- in relation to the CL-containing bilayer, the latter requiring about four times more peptide accumulation to reach the threshold P/L ratio and evidencing the role of membrane curvature strain on the permeabilization process (Lee et al. 2005). The accumulation of peptide required to induce leakage is an important characteristic of the mechanism of action of pore-forming peptides, as proposed by Matsuzaki, Shay e Huang (Matsuzaki 1999; Shay 1999; Huang 2000; Chen et al. 2003). Accordingly, we suggest that when vesicles are homogeneous in size, entrap the same concentration of marker, and the mechanism of action is represented by a sigmoidal concentration dependency, the P/L threshold concentration represents the maximum number of peptide molecules that a membrane can accommodate before breaking and starting to release the vesicle contents as a way of relieving the surface tension (Brochard-Wyart et al. 2000). When this P/L is reached, depending on the bilayer composition, the tension imposed

by bound peptide molecules counterbalances the specific membrane surface tension. This is in good agreement with the findings by Chen et al. (2003) that showed sigmoid concentration dependence between the number of alamethicin molecules occupying the active state of pore formation and P/L concentration ratio, and with the elastic deformation of the membrane caused by bound plus inserted peptide molecules. Another important characteristic is shown in Figs. 2 and 4. The apparent average pore number (p^*) induced by Polybia-MP1 is dependent on the ionic character of the vesicle, at the respective threshold P/L molar ratio, that is, p^* is 0.23 for PC and PCC and 0.15 for PCPG 7030 and PCCL 7030. At each concentration ratio the increased surface tension imposed by the bound peptide molecules reaches a maximum value and leakage starts equally for the anionic or the zwitterionic vesicles, suggesting that the pore structure changes with ionic character of the bilayer, but not with its particular composition.

The MD simulations indicate that Polybia-MP1 assumes an amphipathic α-helical conformation from residue 3 to 13 (Table 2), in TFE/water mixture. The combination of amphiphilicity, electrostatic interactions and backbone solvation, which are not present in MP-X structure, suggests the structural reasons for its selective mode of action. Conformational information obtained from the simulations is in good agreement with the α-helical contents determined in CD spectra. MP-X presented around 61% α-helix in 40% TFE/water mixture (McDowell et al. 1985), corresponding approximately to 8-folded residues. This is the same amount of the most stable hydrogen bonds (i, $i + 4$) as shown in Table 2. In the same environment Polybia-MP-1 presents around 41% α-helix, which corresponds to six helical residues and also to the six most stable (i, $i + 4$) hydrogen bonds throughout the simulation run. Like other mastoparans (Kusunoki et al. 1998; Chuang et al. 1996) Polybia-MP-1 presents unfolded N-terminal residues; in this case it could be also explained by the presence of a hydrogen bond between the charged group of Asp 2 side chain and N of Lys 5 backbone. In MP-X, the same effect comes from the hydrogen bonds between Asn 2 side chain the backbone of residues Lys 4 and Gly 5 (Table 2).

The solvation profile of both peptides shows that the most important difference is the number of water molecules in the region surrounding the C_α. A cylindrical tube-like layer, made of TFE molecules, wraps up the backbone of the peptide chain, protecting the hydrogen bonds and stabilizing the α-helix. Lys charges are located beyond this layer and are solvated by water molecules. In Polybia-MP1, the distribution of charged and polar residues is fundamental for the stability of the helical structure, derived from the equilibrium of electrostatic interactions. This results in a backbone less solvated by TFE than the backbone of MP-X, although both structures are equally stable. These observations are well correlated with the mean hydrophobicity of Polybia-MP1 being lower than that of MP-X (Table 1).

Polybia-MP1 is an interesting antimicrobial peptide due to its highly selective mechanism of action, with low minimum inhibitory concentration (MIC) for Gram-positive and -negative bacteria and no hemolytic activity (Souza et al. 2005). Other mastoparan peptides like MP-X and MP-B, whose primary sequences and structural characteristics present high homology with Polybia-MP1, show intense hemolytic activity (Hirai et al. 1979a; Yu et al. 2000). This important difference in the selectivity of rather similar peptides could be explained by the higher positive charge of MP-B (+5) in relation to all known mastoparans from social wasp venom (Park et al. 1995). In relation to a reference peptide (MP, +4), the hemolytic activity of some mastoparan peptides decreases from MP-B $>$ MP $\gg$ EMP-AF (+4), (Konno et al. 2000) and Polybia MP1(+2) is not hemolytic. According to Dathe et al. (2001), there is a direct relationship between the increase in the positive charge, beyond certain limits, and the development of hemolytic activity. Considering that MP-B, EMP-AF and Polybia MP1 should have comparable low binding levels as deduced from their low helix content in PC vesicles, and looking at their hydrophobicities that decrease from EMP-AF $>$ MP-B $>$ MP1, the lack of hemolytic activity of MP1 could also be attributed to its lower hydrophobicity.

Thus, the selective way of action of Polybia-MP1, in relation MP-B and EMP-AF, can be associated with its lower net charge, associated to a low hydrophobicity as recently proposed in the theoretical model by Taheri-Araghi and Ha (2007). It describes the selective interaction of cationic peptides and membranes, showing the interrelated role of the peptide's charge and its hydrophobicity. Polybia-MP1 has only +2 net charges, but 5 charged residues in total, which agrees with the high-charge requirement for the antimicrobial activity; on the other side, in a zwitterionic bilayer both, the negative and the positive charges, can be electrostatically screened at the head group region and this explains the less hydrophobic environment of the Trp residues. High-charge density requires a larger number of lipids, anionic or zwitterionic, to be counterbalanced causing shrinkage of the optimal head group area of lipids (Taheri-Araghi and Ha 2007), and leading to pore formation.

We suggest that the lack of hemolytic activity of Polybia-MP1 is due to the presence and position of Asp residues that enable the equilibrium of electrostatic interactions (Fig. 7), which is not possible in MP-X and other mastoparans' sequence; this partial neutralization of charges would cause a smaller disturbance of the head group region of zwitterionic lipids in the membrane. A single

substitution of Asp2 residue for Asn2, as occurs in MP-X has led to a hemolytic analog. In this sense, Polybia-MP1 represents a good starting structure whose features might be improved in the search for new therapeutic agents.

Acknowledgments The authors are thankful to Prof. Dr. Joaquim Procopio for his careful reading and suggestions to this manuscript. This work was supported by a grant from the São Paulo State Research Foundation (FAPESP, BIOprospecTA program 04/07942-2); M.P.S.C. has a post doc (154550/2006-0) from the Council for Scientific and Technological Development (CNPq) and received PhD fellowship from CAPES and CNPq. S.T.B.C. received fellowship from CAPES and B.M.S from FAPESP. M.S.P. (Proc. 300377/2003-5) and J.R.N. (310559/2006-5) are CNPq researchers.

References

Allende D, McIntosh TJ (2003) Lipopolysaccharides in bacterial membranes act like cholesterol in eukaryotic plasma membranes in providing protection against melittin-induced bilayer lysis. Biochemistry 42:1101–1108

Allende D, Simon SA, McIntosh TJ (2005) Melittin-induced bilayer leakage depends on lipid material properties: evidence for toroidal pores. Biophys J 88:1828–1837

Andersson A, Danielsson J, Graslund A, Maler L (2007) Kinetic models for peptide-induced leakage from vesicles and cells. Eur Biophys J 36:621–635

Berendsen HJC, Postma JPM, van Gunsteren WF, Hermans J (1981) Interaction models for water in relation to protein hydration. In: Pullman B (ed) Intermolecular forces. Reidel, Dordrecht, pp 331–342

Berendsen HJC, Postma JPM, van Gunsteren W, Di Nola A, Haak JRJ (1984) Molecular dynamics with coupling to an external bath. J Chem Phys 81:3684–3690

Brochard-Wyart F, de Gennes PG, Sandre O (2000) Transient pores in stretched vesicles: role of leak-out. Physica A 278:32–51

Cheatham TE III, Miller JL, Fox T, Darden TA, Kollman PA (1995) Molecular dynamics simulations on solvated biomolecular system: The Particle Mesh Ewald method leads to stable trajectories of DNA, RNA, and proteins. J Am Chem Soc 117:4193–4194

Chen FY, Lee MT, Huang HW (2003) Evidence for membrane thinning effect as the mechanism for peptide-induced pore formation. Biophys J 84:3751–3758

Chuang CC, Huang WC, Yu HM, Wang KT, Wu SH (1996) Conformation of *Vespa basalis* Mastoparan-B in trifluoroethanol-containing aqueous solution. Biochim Biophys Acta 1292:1–8

Dathe M, Schumann M, Wieprecht T, Winkler A, Beyermann M, Krause E, Matsuzaki K, Murase O, Bienert M (1996) Peptide helicity and membrane surface charge modulate the balance of electrostatic and hydrophobic interactions with lipid bilayers and biological membranes. Biochemistry 35:12612–12622

Dathe M, Wieprecht T, Nikolenko H, Handel L, Maloy WL, MacDonald DL, Beyermann M, Bienert M (1997) Hydrophobicity, hydrophobic moment and angle subtended by charged residues modulate antibacterial and haemolytic activity of amphipathic helical peptides. FEBS Lett 403:208–212

Dathe M, Nikolenko H, Meyer J, Beyermann M, Bienert M (2001) Optimization of the antimicrobial activity of Magainin peptides by modification of charge. FEBS Lett 501:146–150

Dos Santos Cabrera MP, de Souza BM, Fontana R, Konno K, Palma MS, de Azevedo Jr WF, Ruggiero Neto J (2004) Conformation and lytic activity of Eumenine Mastoparan: a new antimicrobial peptide from wasp venom. J Peptide Res 64:95–103

Eisenberg D, Schwarz E, Komaromy M, Wall R (1984) Analysis of membrane and surface protein sequences with the hydrophobic moment plot. J Mol Biol 179:125–142

Fioroni M, Burger K, Mark AE, Roccatano D (2000) A new 2,2,2-trifluoroethanol model for molecular dynamics simulations. J Phys Chem B 104:12347–12354

Haines TH, Dencher NA (2002) Cardiolipin: a proton trap for oxidative phosphorylation. FEBS Lett 528:35–39

Heerklotz H, Seelig J (2007) Leakage and lysis of lipid membranes induced by the lipopeptide surfactin. Eur Biophys J 36:305–314

Hess B, Bekker H, Berendsen HJC, Fraaije JGE (1997) LINCS: a linear constraint solver for molecular simulations. J Comp Chem 18:1463–1472

Higashijima T, Burnier J, Ross EM (1990) Regulation of G_i and G_0 by Mastoparan, related amphiphilic peptides and hydrophobic amines. J Biol Chem 265:14176–14186

Hirai Y, Kuwada M, Yasuhara T, Yoshida H, Nakajima T (1979a) A new mast cell degranulating peptide homologous to mastoparan in the venom of Japanese hornet (*Vespa xanthoptera*). Chem Pharm Bull (Tokyo) 27:1945–1946

Hirai Y, Yasuhara T, Yoshida H, Nakajima T, Fujino M, Kitada C (1979b) A new mast cell degranulating peptide "mastoparan" in the venom of *Vespula lewisii*. Chem Pharm Bull (Tokyo) 27:1942–1944

Hori Y, Demura M, Iwadate M, Ulrich AS, Niidome T, Aoyagi H, Asakura T (2001) Interaction of mastoparan with membranes studied by 1H-NMR spectroscopy in detergent micelles and by solid-state 2H-NMR and 15N-NMR spectroscopy in oriented lipid bilayers. Eur J Biochem 268:302–309

Huang HW (2000) Action of antimicrobial peptides: two-state model. Biochemistry 39:8347–8352

Konno K, Hisada M, Naoki H, Itagaki Y, Kawai N, Miwa A, Yasuhara T, Morimoto Y, Nakata Y (2000) Structure and biological activities of Eumenine Mastoparan-AF (EMP-AF), a new mast cell degranulating peptide in the venom of the solitary wasp (*Anterhynchium flavomarginatum micado*). Toxicon 38:1505–1515

Konno K, Hisada M, Fontana R, Lorenzi CCB, Naoki H, Itagaki Y, Miwa A, Kawai N, Nakata Y, Yasuhara T, Ruggiero Neto J, Azevedo Jr WF, Palma MS, Nakajima T (2001) Anoplin, a novel antimicrobial peptide from the venom of the solitary wasp *Anoplius samariensis*. Biochim Biophys Acta 1550:70–80

Kusunoki H, Wakamatsu K, Sato K, Miyazawa T, Kohno T (1998) G protein-bound conformation of mastoparan-X: heteronuclear multidimensional transferred nuclear overhauser effect analysis of peptide uniformly enriched with 13C and 15N. Biochemistry 37:4782–4790

Ladokhin AS, Selsted ME, White SH (1997) Bilayer interactions of Indolicidin, a small antimicrobial peptide rich in tryptophan, proline, and basic amino acids. Biophys J 72:794–805

Ladokhin AS, Jayasinghe S, White SH (2000) How to measure and analyze tryptophan fluorescence in membranes properly, and why bother? Anal Biochem 285:235–245

Lange Y, Dolde J, Steck TL (1981) The rate of transmembrane movement of cholesterol in the human erythrocyte. J Biol Chem 256:5321–5323

Lee MT, Hung WC, Chen FY, Huang HW (2005) Many-body effect of antimicrobial peptides: on the correlation between lipid's spontaneous curvature and pore formation. Biophys J 89:4006–4016

Lindahal E, Hess B, van der Spoel D (2001) Gromacs 3.0: a package for molecular simulations and trajectory analysis. J Mol Model 7:306–317

Lohner K, Prenner EJ (1999) Differential scanning calorimetry and X-ray diffraction studies of the specificity of the interaction of antimicrobial peptides with membrane-mimetic systems. Biochim Biophys Acta 1462:141–156

Matsuzaki K (1999) Why and how are peptide–lipid interactions utilized for self-defense? Magainins and Tachyplesins as archetypes. Biochim Biophys Acta 1462:1–10

Matsuzaki K, Yoneyama S, Murase O, Miyajima K (1996) Transbilayer transport of ions and lipids coupled with mastoparan X translocation. Biochemistry 35:8450–8456

Matsuzaki K, Sugishita K, Ishibe N, Ueha M, Nakata S, Miyajima K, Epand RM (1998) Relationship of membrane curvature to the formation of pores by Magainin 2. Biochemistry 37:11856–11863

McDowell L, Sanyal GB, Prendergast FG (1985) Probable role of amphiphilicity in the binding of mastoparan to calmodulin. Biochemistry 24:2979–2984

Mendes MA, de Souza BM, Palma MS (2005) Structural and biological characterization of three novel mastoparan peptides from the venom of the neotropical social wasp *Protopolybia exigua* (Saussure). Toxicon 45:101–106

Miyamoto S, Kollman PA (1992) SETTLE: an analytical version of the SHAKE and RATTLE algorithm for rigid water models. J Comput Chem 13:952–962

Nakajima T, Uzu S, Wakamatsu K, Saito K, Miyazawa T, Yasuhara T, Tsukamoto Y, Fujino M (1986) Amphiphilic peptides in wasp venom. Biopolymers 25:115–121

Needham D, Nunn RS (1990) Elastic deformation and failure of lipid bilayer membranes containing cholesterol. Biophys J 58:997–1009

Park NG, Yamato Y, Lee S, Sugihara G (1995) Interaction of Mastoparan-B from venom of a hornet in Taiwan with phospholipid bilayer and its antimicrobial activity. Biopolymers 36:793–801

Rohl CA, Baldwin RL (1998) Deciphering rules of helix stability in peptides. Methods Enzymol 295:1–26

Rouser G, Fleischer S, Yamamoto A (1970) Two dimensional thin layer chromatographic separation of polar lipids and determination of phospholipids by phosphorus analysis of spots. Lipids 5:494–496

Schwarz G, Robert CH (1990) Pore formation kinetics in membranes, determined from the release of marker molecules out of liposomes or cells. Biophys J 58:577–583

Schwarz G, Blochmann U (1993) Association of the wasp venom peptide mastoparan with electrically neutral lipid vesicles—salt effects on partitioning and conformational state. FEBS Lett 318:172–176

Shay Y (1999) Mechanism of the binding, insertion and destabilization of phospholipid bilayer membranes by alpha-helical antimicrobial and cell non-selective membrane-lytic peptides. Biochim Biophys Acta 1462:55–70

Shoemaker KR, Kim PS, Brems DN, Marqusee S, York EJ, Chaiken IM, Stewart JM Baldwin RL (1985) Nature of the charged-group effect on the stability of the C-peptide helix. PNAS 82:2349–2353

Souza BM (2007) Estrutura e função de mastoparanos dos venenos de vespas (PhD thesis in Cellular and Molecular Biology) Instituto de Biociências de Rio Claro, UNESP-Universidade Estadual Paulista, Rio Claro, Brasil

Souza BM, Mendes MA, Santos LD, Marques MR, Cesar LM, Almeida RN, Pagnocca FC, Konno K, Palma MS (2005) Structural and functional characterization of two novel peptide toxins isolated from the venom of the social wasp *Polybia paulista*. Peptides 26:2157–2164

Taheri-Araghi S, Ha BY (2007) Physical basis for membrane-charge selectivity of cationic antimicrobial peptides. Phys Rev Lett 98:168101

van Gunsteren WF, Billeter SR, Eising AA, Hünenberger PH, Krüger P, Mark AE, Scott WRP, Tironi IG (1996) Biomolecular simulation: the GROMOS96 manual and user guide; vdf Hochschulverlang: ETH Zürich, Switzerland

Wakamatsu K, Okada A, Miyazawa T, Ohya M, Higashijima T (1992) Membrane-bound conformation of Mastoparan-X, a G-protein-activating peptide. Biochemistry 3:5654–5660

Yeaman MR, Yount NY (2003) Mechanisms of antimicrobial peptide action and resistance. Pharmacol Rev 55:27–55

Yu K, Kang S, Park N, Shin J, Kim Y (2000) Relationship between the tertiary structures of mastoparan B and its analogs and their lytic activities studied by NMR spectroscopy. J Pept Res 55:51–62

Zasloff M (2002) Antimicrobial peptides of multicellular organisms. Nature 415:389–395

Zhao H, Rinaldi AC, Di Giulio A, Simmaco M, Kinnunen PK (2002) Interactions of the antimicrobial peptides temporins with model biomembranes. Comparison of temporins B and L. Biochemistry 41:4425–4436